Precision fringe metrology using a Fresnel zone plate

Chulmin Joo,[a] G. S. Pati, Carl G. Chen, Paul T. Konkola, Ralf K. Heilmann, and Mark L. Schattenburg
Massachusetts Institute of Technology, 77 Mass Avenue, Room 37-432, Cambridge, Massachusetts 02139

Alexander Liddle and Erik H. Anderson
Center for X-ray Optics, Lawrence Berkeley National Laboratory, Berkeley, California 94720

(Received 10 June 2002; accepted 30 September 2002)

In scanning beam interference lithography, a resist-coated substrate is scanned under phase-locked interfering beams to pattern large gratings or grids with nanometer level distortions. To achieve design goals, it is required to measure the spatial period, phase, and rotation of the interference fringes in real-time with high precision. In this article, we report the use of a Fresnel zone plate to characterize interference fringes. With properly controlled errors, it should enable us to achieve high precision measurement of fringe characteristics for a wide range of fringe periods. The mathematical model, details of the metrological procedure, and experimental results are presented. © *2002 American Vacuum Society.* [DOI: 10.1116/1.1523018]

I. INTRODUCTION

The *in situ* measurement of spatial period, phase, and rotation of submicron-period fringes formed by interference of two laser beams is crucial for the successful implementation of scanning beam interference lithography, since it enables the precise stitching of adjacent scans.[1,2] It could also find application in the *in situ* measurement of images in lithography scanners for the purpose of characterizing image overlay.

Previous researchers have attempted to characterize image irradiance distributions by the use of detectors apertured with extremely narrow slits. However, the amount of light leaking through narrow slits decreases dramatically as the deep-submicron-period domain is approached, and aligning the slit with the fringe direction is extremely difficult.

Previously, we proposed to use a beamsplitter for interference fringe metrology.[2] However, the scheme has several limitations, though it proves very effective at measuring the period and the phase of interference fringes. Any distortions in the beamsplitter leads to distortions in the wave fronts of the laser beams, which consequently result in an inaccurate measurement of fringe characteristics. Also, if the interfering beams are rotated to pattern curved gratings,[3] the beamsplitter scheme cannot be used because the transmitted and reflected beams are no longer overlapped. The range in which the beamsplitter can be used is inherently limited. If incident angles vary during operation and become too large or too small, the overlapped beams will no longer be incident on the photodetector. More importantly, the beamsplitter measures the differences in the curvature of the beams, not the fringe phase.

In order to measure phase distortions of an image grating, a fiducial grating can be used. However, this grating metrology necessitates several conditions. For accurate metrology, we need a fiducial grating with high accuracy. Furthermore, it should have the same spatial period as the image grating. If the beams rotate as described before, then the diffracted first and zeroth order beams do not overlap at all.

In this article, a method to characterize interference fringes is proposed by utilizing a Fresnel zone plate. Zone plates are concentric diffractive structures which have a wide range of spatial frequencies. They can be manufactured with very small form factor (typically $\sim 100\ \mu$m in diameter) and high accuracy. Zone plates written by the Lawrence Berkeley National Laboratory (LBNL) NANOWRITER electron-beam lithography tool have a zone placement fidelity of 5 nm in a 131 μm field,[4] which should enable the nano-accurate and high precision characterization of fringes.

Figure 1 demonstrates the Fresnel zone plate metrology scheme. By scanning the zone plate across the interference fringes, their spatial periods can be obtained [Fig. 1(a)]. Interference fringe rotations and distortions can also be detected by moving the zone plate in all directions such as a circular path, which enable us to obtain a phase map of the interference pattern [Fig. 1(b)].

II. THEORETICAL MODEL

Let us consider two unit-amplitude monochromatic plane waves incident upon a zone plate (Fig. 2). The plane waves are assumed to have different incident angles, so they are given by

$$f_1(x,y) = \exp\left(i \frac{2\pi}{\lambda} \sin\theta_1 x \right), \tag{1}$$

$$f_2(x,y) = \exp\left(-i \frac{2\pi}{\lambda} \sin\theta_2 x \right). \tag{2}$$

Here λ is the wavelength of light, and θ_1 and θ_2 are the incident angles of two plane waves relative to the z axis. For convenience, the time dependent factor $\exp(i\omega t)$ has been dropped. If two plane waves are interfered to form an image grating on the (x,y) plane (Fig. 3), its intensity is given by

[a]Electronic mail: cmjoo@mit.edu

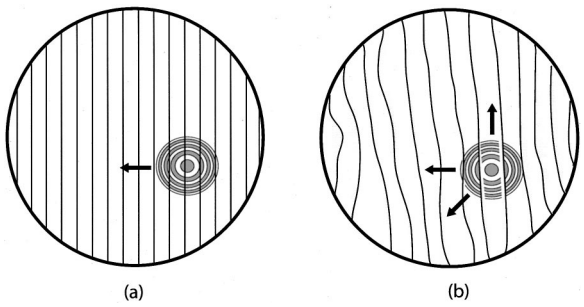

FIG. 1. Interference fringe metrology scheme: (a) interference fringe period measurement and (b) interference fringe mapping.

$$I_g(x,y)=2+2\cos\left(\frac{2\pi}{\Lambda}x\right), \tag{3}$$

where

$$\Lambda=\frac{\lambda}{\sin\theta_1+\sin\theta_2}.$$

Hence, the image grating has a period of Λ in the (x,y) plane.

A zone plate is a circularly symmetric diffraction grating composed of alternate transparent and opaque annular zones. It is periodic in radius squared, and its center is assumed to be shifted by ϵ relative to the origin as shown in Fig. 3. Then, its transmittance can be expressed by a Fourier series[5]

$$t(x,y)=\sum_{n=-\infty}^{\infty}A_n\exp\left(in\pi\frac{(x-\epsilon)^2+y^2}{\rho_0^2}\right), \tag{4}$$

where ρ_0 is a constant and equal to the radius of the first zone for a conventional Fresnel zone plate. Since the transmittance must be real, $A_n=A_{-n}^{*}$.

As mentioned before, if two plane waves are incident upon the zone plate, they are diffracted and interfered on the (x',y') plane, which is parallel to the (x,y) plane and at normal distance z from it. With the assumption[6]

$$z\gg\frac{\pi D^2}{4\lambda},$$

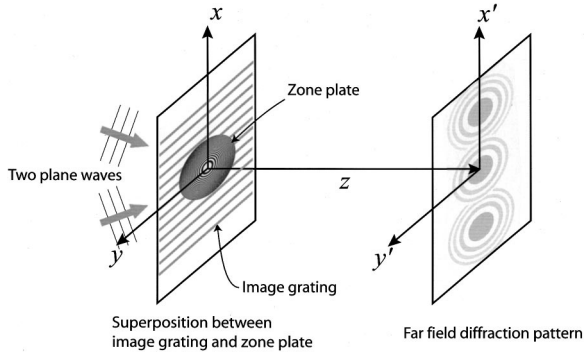

FIG. 2. Diffraction geometry of a Fresnel zone plate and two plane waves.

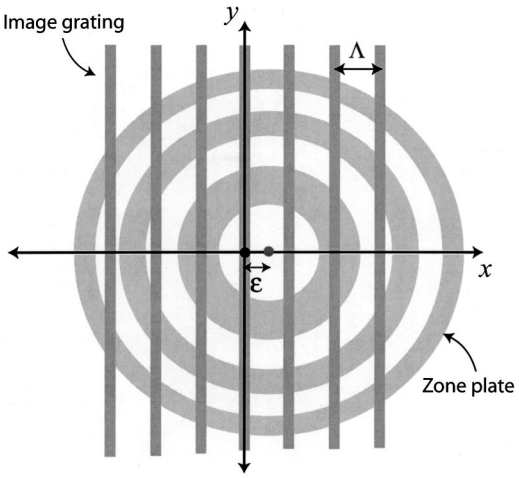

FIG. 3. Image grating and a Fresnel zone plate on the (x,y) plane.

where D is the diameter of the zone plate, the field distribution $u(x',y')$ across the (x',y') plane can be evaluated using the Fraunhofer diffraction approximation as below:

$$u(x',y')=\frac{\exp\left(i\frac{2\pi}{\lambda}z\right)\exp\left(\frac{i\pi}{z\lambda}(x'^2+y'^2)\right)}{i\lambda z}\times\int\int_{-\infty}^{\infty}t(x,y)\{f_1(x,y)+f_2(x,y)\}\times\exp\left(-i\frac{2\pi}{\lambda z}(xx'+yy')\right)dx\,dy. \tag{5}$$

Aside from multiplicative phase factors preceding the integral, Eq. (5) is simply the Fourier transform of $t(x,y)\times(f_1(x,y)+f_2(x,y))$, evaluated at frequencies $(x'/\lambda z,y'/\lambda z)$. Let $\mathcal{F}$ denote the Fourier transform. Then, Eq. (5) can be expressed as

$$u(x',y')=\frac{\exp\left(i\frac{2\pi}{\lambda}z\right)\exp\left(\frac{i\pi}{z\lambda}(x'^2+y'^2)\right)}{i\lambda z}\times[\mathcal{F}\{f_1(x,y)\}+\mathcal{F}\{f_2(x,y)\}]\otimes\mathcal{F}\{t(x,y)\}, \tag{6}$$

where the symbol $\otimes$ represents convolution operator. Using

$$\mathcal{F}\{f_1(x,y)\}=\delta\left(\frac{x'}{\lambda z}-\frac{\sin\theta_1}{\lambda},\frac{y'}{\lambda z}\right),$$

$$\mathcal{F}\{f_2(x,y)\}=\delta\left(\frac{x'}{\lambda z}+\frac{\sin\theta_2}{\lambda},\frac{y'}{\lambda z}\right),$$

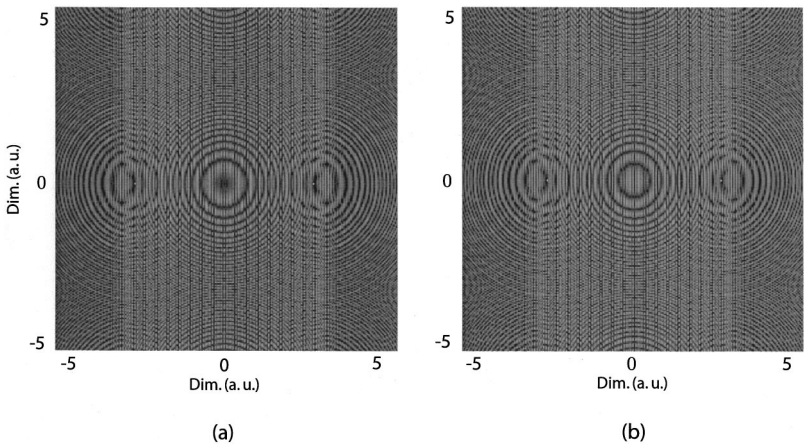

FIG. 4. Simulated far-field diffraction pattern of two plane waves by a Fresnel zone plate with diameter of innermost zone/image grating period = 10.

$$\mathcal{F}\{t(x,y)\} = i\rho_0^2 \sum_{n=-\infty}^{\infty} \frac{A_n}{n} \times \exp\left[-i \frac{\pi \rho_0^2}{n} \left(\left(\frac{x'}{\lambda z} \right)^2 + \left(\frac{y'}{\lambda z} \right)^2 \right) \right] \times \exp\left(-i 2\pi \frac{x'}{\lambda z} \epsilon \right),$$

and assuming, for convenience, that any point on the (x',y') plane can be characterized by a two-dimensional vector $\mathbf{r} = (x'/\lambda z, y'/\lambda z)$, Eq. (5) is expressed as

$$u(\mathbf{r}) = \frac{\exp\left(i \frac{2\pi}{\lambda} z \right) \exp\left(\frac{i\pi}{z\lambda} (x'^2 + y'^2) \right)}{i\lambda z} \times \left\{ g_1(\mathbf{r}) \exp\left(-i 2\pi \frac{\sin\theta_1}{\lambda} \epsilon \right) + g_2(\mathbf{r}) \exp\left(i 2\pi \frac{\sin\theta_2}{\lambda} \epsilon \right) \right\}, \quad (7)$$

where

$$g_1(\mathbf{r}) = i\rho_0^2 \sum_{m=-\infty}^{\infty} \frac{A_m}{m} \exp\left(-\frac{i\pi\rho_0^2}{m} |\mathbf{r} - \mathbf{r}_1|^2 \right),$$

$$g_2(\mathbf{r}) = i\rho_0^2 \sum_{n=-\infty}^{\infty} \frac{A_n}{n} \exp\left(-\frac{i\pi\rho_0^2}{n} |\mathbf{r} - \mathbf{r}_2|^2 \right),$$

$$\mathbf{r}_1 = (\sin\theta_1/\lambda, 0),$$

$$\mathbf{r}_2 = (-\sin\theta_2/\lambda, 0).$$

Since $g_1(\mathbf{r})$ and $g_2(\mathbf{r})$ are real, the intensity across the (x',y') plane is given by

$$I(\mathbf{r}) = u(\mathbf{r})u(\mathbf{r})^* = \frac{1}{\lambda^2 z^2} \left[g_1(\mathbf{r})^2 + g_2(\mathbf{r})^2 + 2\cos\left(\frac{2\pi}{\Lambda} \epsilon \right) g_1(\mathbf{r}) g_2(\mathbf{r}) \right]. \quad (8)$$

Equation (8) is composed of three terms: two squared linear combinations of quadratic phase exponentials and the superposition of $g_1(\mathbf{r})$ and $g_2(\mathbf{r})$ modulated by a cosine function of ϵ with a period Λ. The $g_1(\mathbf{r})^2$ and $g_2(\mathbf{r})^2$ terms correspond to the far-field diffraction patterns of the zone plate under illuminations from two plane waves, so we will call them the far-field zone plates (FFZPs) from now on. Also, the third term in Eq. (8) is the pattern formed by the superposition of FFZPs, $g_1(\mathbf{r})$ and $g_2(\mathbf{r})$, and will be called the far-field moiré zone plates (FMZPs). The FMZPs have multiple orders, and the first order FMZP, which has the highest irradiance, is located between the centers of $g_1(\mathbf{r})^2$ and $g_2(\mathbf{r})^2$. If $g_1(\mathbf{r})^2$ and $g_2(\mathbf{r})^2$ are located with small separation of their centers, the FMZPs become linear fringes.[5]

For interference fringe metrology, we are interested in the FMZPs since they are modulated by the cosine function as described above. If intensity given by Eq. (8) is integrated over an arbitrary area on the (x',y') plane, optical power is obtained, and it is a sinusoidal function of the displacement of the zone plate with the same period as the image grating. Therefore, by moving a zone plate across the interference fringes, fringe period and phase can be obtained.

Figure 4 shows simulation results for the far-field irradiance distribution produced by an image grating transmitted through a Fresnel zone plate. Note that the phase of the first order FMZP, shown in Fig. 4(a), changes by π when the zone plate is displaced by one half of the period of the image grating, shown in Fig. 4(b).

III. EXPERIMENT

Figure 5 depicts a schematic of the experimental setup. A Fresnel zone plate is mounted on top of a translation stage, which is driven by a New Focus Model 8302 picomotor. Figure 6 shows a scanning electron microscope (SEM) micrograph of the amplitude Fresnel zone plate which is used throughout the experiment. It has 200 zones, a minimum zone width of 207 nm, and a diameter of 127 μm. Due to the nondeterministic motion of the picomotor, the displacement traveled by the stage is measured using a capacitance gauging instrument (ADETech., Model 4810) which has a resolu-

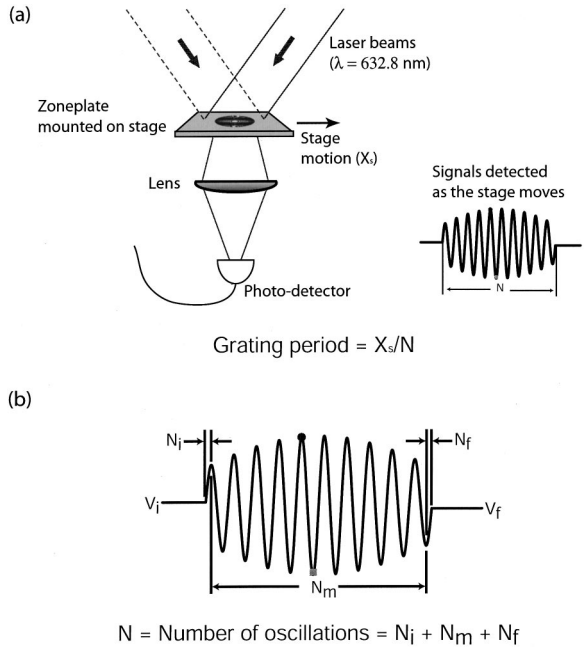

FIG. 5. (a) Interference fringe metrology using a Fresnel zone plate and (b) oscillation counting.

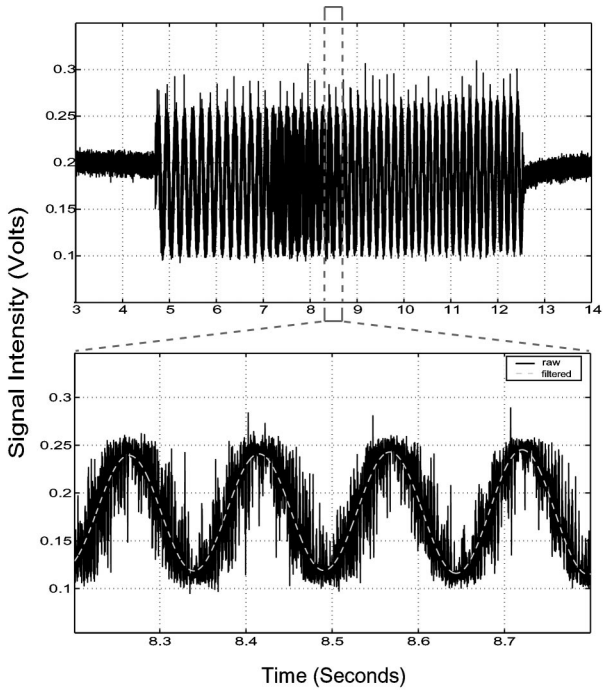

FIG. 7. Raw and digitally filtered signals (sample rate = 5 kHz, angle of incidence = 20°).

tion of 0.1 nm and a linearity of ±0.05%. Two coherent laser beams ($\lambda = 632.8$ nm, diameter≈2 mm) are incident upon the Fresnel zone plate and diffracted to form the far-field patterns on the lens. The lens is positioned to sample the first order FMZP and focus it onto a photodiode. It is located at a distance z of 10 cm from the Fresnel zone plate, which is in the Fraunhofer regime.

As the Fresnel zone plate is scanned across the interference fringes, optical power is measured at the photodiode. As mentioned, optical power is a sinusoidal function of the displacement of the Fresnel zone plate with the same period as the interference fringes. Therefore, the interference fringe period and phase can be derived directly from the number of oscillations of the signal observed at the photodiode, N, and knowledge of the distance traveled by the translation stage, X_s. In other words, the signal completes one cycle of oscillation as the stage traverses one fringe period. Thus, by dividing the distance traveled by the translation stage by the total number of oscillations observed at the photodiode, the period of interference fringes can be derived. A National Instruments NI 6043E I/O board is used for A/D conversion. The total number of oscillations is the sum of three terms as illustrated in Fig. 5(b). Knowledge of the initial and final signal levels and number of peaks and valleys is a necessary condition for precise determination of the number of oscillations.

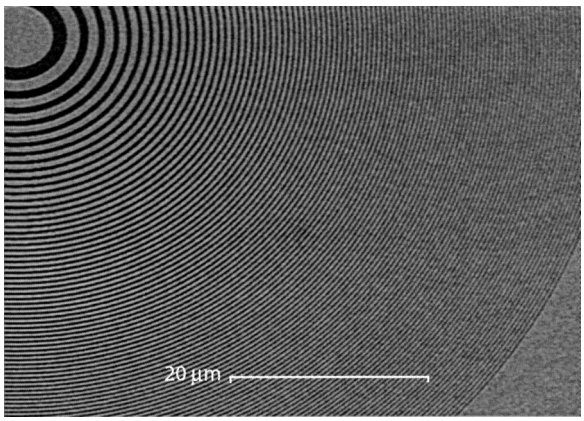

FIG. 6. SEM micrograph of the amplitude Fresnel zone plate written by LBNL NANOWRITER. It has 200 zones, a minimum zone width of 207 nm, and a diameter D of 127 μm.

IV. EXPERIMENTAL RESULTS AND DISCUSSIONS

Thirty sets of period measurements for incident angles of 20° and 35° were carried out. Figure 7 shows signals sampled at the photodiode as the translation stage was displaced for an incident angle of 20°. The sample rate is at 5 kHz. A lot of noise was present primarily due to acoustics and excitation from internal vibrations of the picomotor. For accurate detection of oscillations, the signals were filtered using a finite impulse response (FIR) low-pass filter (Kaiser Window) with a cutoff frequency of 10 Hz, a transition band of 15 Hz, and ⩾60 dB attenuation in the stop band. The filtered signal is shown in Fig. 7. With the knowledge of number of oscillations N and the distance traveled by the translation stage X_s, interference fringe periods were calculated for each case. The oscillation counting program was implemented using MATLAB.

A protractor with a resolution of 1° was used to measure incident angles. The predicted fringe periods are 925.9 ±44.3 nm for an incident angle of 20° and 551.6±13.7 nm

for an incident angle of 35°. From the period measurements, the mean fringe periods of 911.8 and 541.1 nm were obtained, respectively. The one-sigma repeatabilities were 1.1 and 0.9 nm for each case. The poor resolution of the angle measurement is a significant contributor to the discrepancy between the predicted and the measured periods.

The period measurement uncertainty involves several factors. The inaccuracy of the capacitance sensor corresponds to an uncertainty of ± 0.32 nm for an incident angle of 20° and ± 0.23 nm for an incident angle of 35°. Since this uncertainty is proportional to $1/N$, it can be reduced further by long travel of the translation stage, thereby increasing the number of oscillations N. Cosine errors in the alignment of the Fresnel zone plate, displacement sensor, and the interferometric optics result in bias errors. The Fresnel zone plate was set to travel normal to the image grating lines within 0.5 mrad, which corresponds to an uncertainty of ± 0.6 and ± 0.2 nm for each case. The 1° misalignment of the translation stage with the zone plate plane leads to an error of 0.015% of the actual period. The inaccurate count of the number of oscillations is also an error source. For the average values of N and X_s, inaccurate detection of 1/4 oscillation leads to an uncertainty of ± 4.7 nm for an incident angle of 20° and ± 1.9 nm for an incident angle of 35°. This error decreases by $1/N^2$.

Furthermore, the repeatability suffers from many error sources, including fringe drift due to the change of refractive index, vibrations, and acoustics. It can be improved by averaging a larger amount of sampled data. Note that the experiments have been performed without a properly designed low coefficient of thermal expansion metrology frame, a fringe locker, or an environmental control.

V. CONCLUSION

A method for *in situ* interference fringe metrology using a Fresnel zone plate was presented. Through the optical power measurement of the far-field irradiance produced by an image grating and a Fresnel zone plate, the interference fringe periods were obtained. This scheme can be used for a wide range of fringe periods, and should enable achievement of subnanometer fringe characterization with corrected error sources. Studies about contrast variations with changing fringe period are underway.

ACKNOWLEDGMENTS

The authors gratefully acknowledge the outstanding technical assistance of Robert Fleming and Edward Murphy. Student, staff, and facility support from the Space Nanotechnology Laboratory are also appreciated. This work was supported by DARPA under Grant No. DAAG55-98-1-0130 and NASA under Grant No. NAG5-5271.

[1]M. L. Schattenburg, C. Chen, P. N. Everett, J. Ferrera, P. Konkola, and H. I. Smith, J. Vac. Sci. Technol. B **17**, 2692 (1999).
[2]C. G. Chen, P. T. Konkola, R. K. Heilmann, G. S. Pati, and M. L. Schattenburg, J. Vac. Sci. Technol. B **19**, 2335 (2001).
[3]G. S. Pati *et al.*, J. Vac. Sci. Technol. B (submitted)
[4]Erik H. Anderson *et al.*, J. Vac. Sci. Technol. B **18**, 2970 (2000).
[5]G. Harburn, T. R. Welberry, and R. P. Williams, in *Selected Papers on Zone Plates*, SPIE Milestone Series, edited by J. Ojeda-Castaneda and C. Gomez-Reino (SPIE, Bellingham, WA, 1996), p. 242.
[6]J. W. Goodman, *Introduction to Fourier Optics*, 2nd ed (McGraw–Hill, Boston, MA, 1996).